

Implementing quantum Ricci curvature

N. Klitgaard* and R. Loll†

*Institute for Mathematics, Astrophysics and Particle Physics, Radboud University,
Heyendaalseweg 135, 6525 AJ Nijmegen, The Netherlands*



(Received 28 February 2018; published 21 May 2018)

Quantum Ricci curvature has been introduced recently as a new, geometric observable characterizing the curvature properties of metric spaces, without the need for a smooth structure. Besides coordinate invariance, its key features are scalability, computability, and robustness. We demonstrate that these properties continue to hold in the context of nonperturbative quantum gravity, by evaluating the quantum Ricci curvature numerically in two-dimensional Euclidean quantum gravity, defined in terms of dynamical triangulations. Despite the well-known, highly nonclassical properties of the underlying quantum geometry, its Ricci curvature can be matched well to that of a five-dimensional round sphere.

DOI: [10.1103/PhysRevD.97.106017](https://doi.org/10.1103/PhysRevD.97.106017)

I. QUANTUM GRAVITY NEEDS MORE OBSERVABLES

Suppose quantum gravity and spacetime at the Planck scale can be described by local dynamical degrees of freedom, which are geometric in the sense that (quantum analogues of) geodesic distances and volumes exist. We are primarily interested in situations where, unlike in general relativity, there is no *a priori* differentiable manifold M and smooth metric structure $g_{\mu\nu}(x)$ present, and standard tensor calculus is therefore not available. Can we nevertheless describe quantum spacetime in terms of generalized geometry, and on sufficiently large scales recover the usual notions of classical geometry?

Quantum gravity from causal dynamical triangulations (CDT) is a framework of this kind, where moreover such questions can be addressed explicitly and quantitatively, and some have already been answered in the affirmative (see Ref. [1] for a review). Roughly speaking, “quantum spacetime” in this setting arises from a suitable scaling limit of a gravitational path integral. The latter takes the form of a weighted superposition of piecewise flat spacetimes, which serve as regulated approximations of curved spacetime geometries of a given fixed topology.

Any analysis of the physical content of such a candidate theory of quantum gravity has to be made in terms of observables. In the covariant context we are considering,

observables are purely geometric functions of the dynamical variables that do not depend on spacetime labels, a requirement that in classical gravity is usually phrased as “invariance under diffeomorphisms”.¹ However, the observation that “a scalar function $\phi(x)$ cannot be an observable because it depends on the spacetime label x ” is independent of whether x takes discrete, continuous, or smooth values. To eliminate the dependence on unphysical spacetime labels or coordinates one can average or integrate over them. For example, nonlocal observables in classical gravity can be obtained by integrating curvature scalars over spacetime. In a similar spirit, one may construct diffeomorphism-invariant two-point functions in quantum gravity by integrating over all pairs of points with a given geodesic distance between them (see Ref. [2] for an example).

The general challenge in nonperturbative quantum gravity without a background metric structure, smooth or otherwise, is to construct what we will call *good quantum observables*. Apart from being geometric, they are defined to be scalable, that is, associated with a variable distance scale δ , and their expectation values should be computable, finite, and not identically zero. Last, they should have a well-defined classical limit for sufficiently large δ . Although for small δ such an observable $\mathcal{O}(\delta)$ will characterize spacetime properties at short distances, it will not be local in the usual sense, because the definition of $\mathcal{O}(\delta)$ will typically involve an integration over spacetime, as noted above.

The rather striking results that have come out of CDT quantum gravity—including the emergence of de Sitter space [3], the crucial role of causal structure [4], and the phenomenon of dynamical dimensional reduction [5]—have been based on the study of just four geometric

*n.klitgaard@science.ru.nl

†r.loll@science.ru.nl

Published by the American Physical Society under the terms of the Creative Commons Attribution 4.0 International license. Further distribution of this work must maintain attribution to the author(s) and the published article’s title, journal citation, and DOI. Funded by SCOAP³.

¹Note that we are not dealing with so-called Dirac observables, which appear in canonical formulations of general relativity.

observables: the spectral and Hausdorff dimensions, the total spatial volume as a function of cosmological proper time (i.e., the global shape of the universe), and quantum fluctuations of the latter. However, more observables are clearly needed, for example, to understand the nature of the newly found phase transition [6], to improve the existing renormalization group analysis [7], and to quantify (Planckian) physics near the already found second-order phase transitions [8].

To improve on this situation, we recently introduced a new observable, the *quantum Ricci curvature*, and investigated some of its properties on smooth and piecewise flat classical spaces [9]. Building on these results, which will be summarized in Sec. II, we present in Sec. III the first genuine quantum implementation of quantum Ricci curvature, namely, in two-dimensional quantum gravity formulated in terms of dynamical triangulations (DT), the Euclidean precursor of CDT (see Ref. [10] for an introduction).

DT quantum gravity is an excellent testing ground for our prescription. First, in the context of nonperturbative quantum gravity, the important role of the *Hausdorff dimension* in characterizing the universal, intrinsic properties of quantum geometry was highlighted first in pioneering work in two-dimensional DT [11,12]. This quantity is a prime example of a good quantum observable in our sense, in any dimension. Second, as also revealed by this early work, the quantum geometry obtained in this model is fractal and highly nonclassical (with Hausdorff dimension $d_H = 4$), and its behavior is dictated by the dynamics of branching baby universes on all scales. It will be particularly interesting to understand to what extent the quantum Ricci curvature will reflect the pure quantum nature of the underlying geometry.

II. QUANTUM RICCI CURVATURE

Since Ricci curvature in the continuum is a two-tensor, the question arises how its inherent directional dependence can be captured in a nonsmooth context. We will associate the Ricci curvature $\text{Ric}(v, v) = R_{ij}v^i v^j$ along a vector v with a quasilocal construction involving a pair of overlapping geodesic spheres. Note that because of its symmetry the Ricci tensor $R_{ij}(x)$ is determined completely by evaluating it on pairs of identical vectors.

Our definition of quantum Ricci curvature [9] is inspired by Ollivier’s coarse Ricci curvature [13], but uses a different notion of sphere distance, which is essential for the application in quantum gravity.² The crucial quantity to

²Note that our construction is applicable to metric spaces of positive-definite signature, like in the Euclidean quantum gravity model considered below, or in CDT quantum gravity after applying the “Wick rotation” of that formulation [1]. There is no immediate Lorentzian analogue of our quantum Ricci curvature construction, which presumably would involve (infinitely extended) hyperboloids rather than spheres of radius δ .

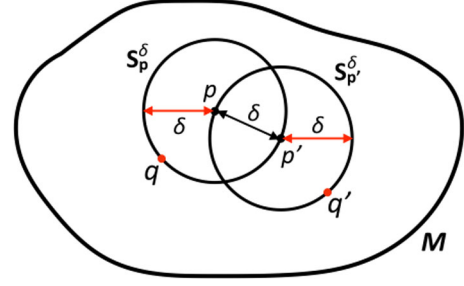


FIG. 1. Two overlapping δ -spheres, whose centers p and p' are a distance δ apart. Determining the quasilocal quantum Ricci curvature associated with this configuration involves averaging over the distances between all point pairs (q, q') along the circles.

compute is the average sphere distance \bar{d} of two overlapping spheres S_p^δ and $S_{p'}^\delta$ of radius δ , whose centers p and p' are a geodesic distance δ apart, as illustrated in Fig. 1. On a D -dimensional Riemannian manifold, for sufficiently small δ , \bar{d} is given by the normalized integral over the two spheres,

$$\bar{d}(S_p^\delta, S_{p'}^\delta) := \frac{1}{\text{vol}(S_p^\delta)} \frac{1}{\text{vol}(S_{p'}^\delta)} \times \int_{S_p^\delta} d^{D-1} q \sqrt{h} \int_{S_{p'}^\delta} d^{D-1} q' \sqrt{h'} d(q, q'), \quad (1)$$

where h and h' are the determinants of the metrics induced on S_p^δ and $S_{p'}^\delta$, and $d(q, q')$ denotes the geodesic distance between the points q and q' . The important feature of Eq. (1) is that it can be generalized to nonsmooth metric spaces and be computed in a straightforward way. A δ -sphere S_p^δ around p will in this case be interpreted as the set of all points q with distance δ from p . Given \bar{d} , the dimensionless quantum Ricci curvature $K_q(p, p')$ is defined via

$$\frac{\bar{d}(S_p^\delta, S_{p'}^\delta)}{\delta} = c_q(1 - K_q(p, p')), \quad \delta = d(p, p'), \quad (2)$$

where c_q is a positive constant, which depends on the metric space under consideration, and K_q captures any nontrivial dependence on δ .

Although our interest is in the nonsmooth case and noninfinitesimal δ , Eq. (2) can just as well be evaluated on a general smooth D -dimensional Riemannian manifold in the limit as $\delta \rightarrow 0$. Using Riemann normal coordinates based at the point p , say, and expressing the result as a power series in δ , one finds in dimensions $D = 2, 3$, and 4

$$\frac{\bar{d}}{\delta} = \begin{cases} 1.5746 + \delta^2(-0.1440 \text{Ric}(v, v) + \mathcal{O}(\delta)), & D = 2, \\ 1.6250 + \delta^2(-0.0612 \text{Ric}(v, v) - 0.0122 R + \mathcal{O}(\delta)), & D = 3, \\ 1.6524 + \delta^2(-0.0469 \text{Ric}(v, v) - 0.0067 R + \mathcal{O}(\delta)), & D = 4, \end{cases} \quad (3)$$

where v denotes the unit vector at p in the direction of p' and R is the Ricci scalar (trace of the Ricci tensor) at p . The various coefficients in Eq. (3) arise from the numerical evaluation of exact integral expressions, which depend on D but not on the geometry.³

Let us emphasize that we follow the same logic as standard lattice field theory with regard to regularization, renormalization, and continuum limit. This implies that we are not interested in finite structures (like triangulations or other polygonizations of spacetime) *per se*, but only in suitable infinite limits associated with potential quantum gravity theories, where most lattice details will become irrelevant. An important outcome of our analysis of quantum Ricci curvature on various piecewise flat spaces [9] was that these so-called lattice artifacts appear to be confined to a region $\delta \lesssim 5$, with δ measured in discrete link units.

III. THE CURVATURE OF DT QUANTUM GRAVITY IN TWO DIMENSIONS

Two-dimensional Euclidean quantum gravity can be defined as the scaling limit of the nonperturbative path integral [10]

$$Z(\lambda) = \sum_{T \in \mathcal{T}} \frac{1}{C_T} e^{-S[T]}, \quad S[T] = \lambda N(T), \quad (4)$$

where λ denotes the (bare) cosmological constant. The triangulations T summed over in Eq. (4) are two-dimensional simplicial manifolds of spherical topology, made of equilateral triangles, and C_T denotes the order of the automorphism group of T . The Einstein-Hilbert action S reduces to a cosmological term proportional to the (discrete) volume of a configuration T , namely, the number $N(T)$ of triangles contained in T .⁴ A common choice, which we will also adopt here, is to work with a particular discrete notion of geodesic distance. It is measured only between pairs (q, q') of vertices, where $d(q, q')$ equals the number of edges of the shortest path between q and q' , and is therefore also integer valued. In line with our remarks at the end of Sec. II, the details of these discretization choices (and others made below) should not matter in the continuum limit.

³Note that in $D = 2$, the Ricci curvature and Ricci scalar coincide up to a factor of 2.

⁴The number of edges is $N_1(T) = \frac{3}{2}N(T)$ and the number of vertices is $N_0(T) = \frac{1}{2}N(T) + 2$.

The analogue of the average sphere distance on triangulations is given by

$$\bar{d}(S_p^\delta, S_{p'}^\delta) = \frac{1}{N_0(S_p^\delta)} \frac{1}{N_0(S_{p'}^\delta)} \sum_{q \in S_p^\delta} \sum_{q' \in S_{p'}^\delta} d(q, q'), \quad (5)$$

where $N_0(S_p^\delta)$ denotes the number of vertices at distance δ from the vertex p . Because of the branching baby-universe structure of typical DT configurations, the δ -“spheres” S^δ we defined earlier below Eq. (1) will in general be multiply connected, even for small δ . One way of making Eq. (5) into a “classical” observable is by averaging it over all point pairs,

$$\bar{d}_T(\delta) = \frac{1}{n_T(\delta)} \sum_{p \in T} \sum_{p' \in T} \bar{d}(S_p^\delta, S_{p'}^\delta) \delta_{d(p, p'), \delta}, \quad (6)$$

where the Kronecker delta δ enforces the distance δ between p and p' , and $n_T(\delta)$ denotes the number of point pairs (p, p') in T with $d(p, p') = \delta$. Note that Eq. (6) includes an average over directions of the quasilocal quantum Ricci curvature.

The quantity we have studied with the help of Monte Carlo simulations is the (normalized) expectation value $\bar{d}(\delta)/\delta := \langle \bar{d}_T(\delta) \rangle_N / \delta$ in the DT ensemble of Eq. (4), for fixed volume N , and specifically its behavior as $N \rightarrow \infty$. We used a Metropolis algorithm, with updates by so-called flip moves, consisting in flipping the inner edge of a pair of adjacent triangles; see Fig. 2. This move is ergodic in the set of triangulations of fixed topology and fixed volume (see, for example, Ref. [10]). It is always accepted when the algorithm proposes it, provided the resulting triangulation satisfies the local simplicial manifold conditions.

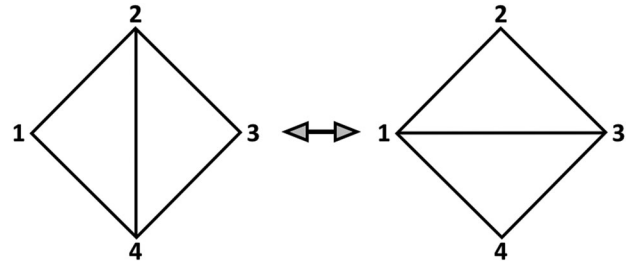


FIG. 2. The flip move changes the local geometry of a two-dimensional triangulation by substituting a pair of adjacent triangles, (1,2,4) and (2,3,4), by the triangle pair (1,2,3) and (1,3,4), or vice versa.

For fixed volume N , we performed a double-sampling of \bar{d}/δ over geometries and point pairs, where a single measurement consists of the following steps: (i) pick a random vertex $p \in T$ in the triangulation T that has been generated at this stage of the Metropolis algorithm; (ii) pick a vertex p' randomly from the sphere of radius $\delta = 1$ around p and compute $\bar{d}(S_p^\delta, S_{p'}^\delta)/\delta$; (iii) repeat step (ii) for the same p and a randomly chosen point p' from the δ -sphere around p , for $\delta = 2, 3, \dots, 15$, yielding a total of 15 data points for T . Sweeps between measurements consisted of 4×10^7 suggested updates each. We performed 100 000 measurements at volume $N = 20k$, 80 000 at $N = 30k$, and 20 000 each at $N = 40, 60, 80, 120, 160$, and $240k$.

To start with, we wanted to understand whether the measured normalized average sphere distance $\bar{d}(\delta)/\delta$ shows any qualitative resemblance with the behavior of a smooth manifold of constant (sectional) curvature, at least for some range of δ . Spherical, hyperbolic, and flat spaces serve as convenient references because of the distinct behavior of their quantum Ricci curvature K_q , extracted from $\bar{d}(\delta)/\delta = c_q(1 - K_q(\delta))$, as illustrated by Fig. 3. Note that our *a priori* choice of spherical topology for the triangulations T does not impose any obvious topological constraints on $K_q(\delta)$, since the quantum Ricci curvature does not satisfy a Gauss-Bonnet theorem for any value of δ . At any rate, it is unclear what the physical status of such a theorem would be in a theory where we already know that in the scaling limit the dynamically generated quantum geometry bears little resemblance to a classical two-dimensional Riemannian manifold.

Figure 4 shows the measured expectation values of the normalized average sphere distance \bar{d}/δ , taken at volume

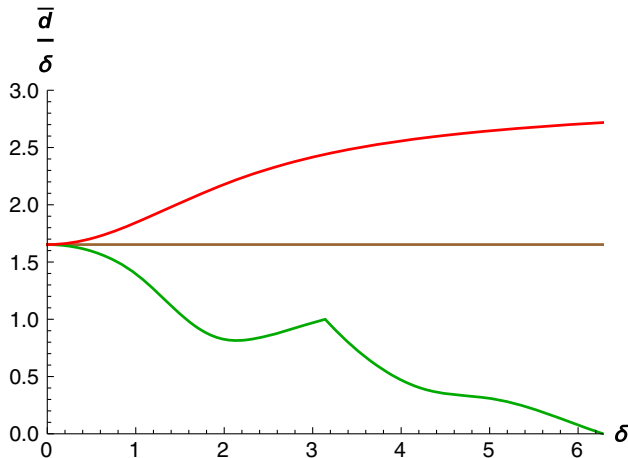


FIG. 3. The normalized average sphere distance \bar{d}/δ , as a function of the scale $\delta \in [0, 2\pi]$, for three constantly curved manifolds in four dimensions: hyperbolic, with $K_q < 0$ (top); flat, with $K_q = 0$ (middle); spherical, with $K_q > 0$ (bottom). The curvature radius ρ of the nonflat spaces has been set to 1. The curves in other dimensions D are qualitatively very similar [9].

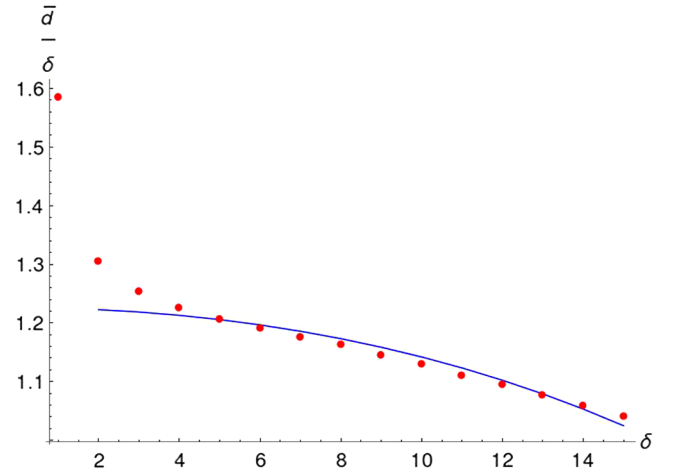


FIG. 4. Expectation value of the normalized average sphere distance \bar{d}/δ in dynamical triangulations at volume $N = 40k$, as a function of the link distance δ , and the best fit of the data for $\delta > 5$ to a continuum sphere of dimension $D = 4^5$ (continuous curve) and curvature radius $\rho = 16.7$. (Error bars are smaller than dot size.)

$N = 40k$. For small δ , approaching the minimal value $\delta = 1$, we observe a rapid increase in \bar{d}/δ . This seems to be the same short-distance effect we found for $\delta \lesssim 5$ for all of the piecewise flat geometries investigated in Ref. [9], *irrespective of their behavior for larger δ* , and which we have already identified as a discretization artifact. For $\delta \gtrsim 5$, we enter a region of gentler, monotonic decrease, suggestive of a positive quantum Ricci curvature, corresponding to the initial section of the bottom curve in Fig. 3.

This motivated our next step: a systematic quantitative comparison of the measured data for $\langle \bar{d}/\delta \rangle$ with the corresponding curves for continuum spheres of constant curvature. In view of the fact that the spectral dimension of DT quantum gravity is $d_S = 2$ and its Hausdorff dimension $d_H = 4$, we have performed fits to spheres with a range of dimensions, $D = 2, 3, 4$, and 5 . Unlike in the continuum, where the constant $c_q^{\text{cont}} := \lim_{\delta \rightarrow 0} \bar{d}/\delta$ of Eq. (2) is universal, as already mentioned in Sec. II, we established in Ref. [9] that the same is not true in the realm of piecewise flat spaces, where we have identified $c_q \equiv (\bar{d}/\delta)|_{\delta=5}$. Using the same identification for the DT data, a relative shift between continuum and lattice data is needed to account for the different values of c_q . Following Ref. [9], we require all curves to go through the point at $\delta = 5$ and use two alternative methods to achieve this: a relative additive shift and a relative multiplicative shift between the continuum and DT data for \bar{d}/δ .

After fixing the relative shift for a data set at given volume N , we determine the remaining free parameter,

⁵It will presently become clear why we are not interested exclusively in $D = 2$. The analogous curves in two, three, and five dimensions are qualitatively similar.

TABLE I. Effective curvature radii ρ_{eff} obtained from fitting Monte Carlo data to smooth spheres in various dimensions D , using both additive (“+”) and multiplicative (“ \times ”) shifts, and system sizes of up to $N = 240k$.

N	$D = 2, +$	$D = 2, \times$	$D = 3, +$	$D = 3, \times$	$D = 4, +$	$D = 4, \times$	$D = 5, +$	$D = 5, \times$
$20k$	12.94(2)	11.805(15)	14.04(2)	12.49(2)	14.68(3)	12.86(2)	15.02(3)	13.07(2)
$30k$	13.67(2)	12.52(2)	15.04(3)	13.37(2)	15.76(4)	13.82(3)	16.16(4)	14.06(3)
$40k$	14.28(6)	13.09(5)	15.93(8)	14.08(6)	16.71(9)	14.61(7)	17.14(8)	14.89(6)
$60k$	15.15(9)	13.81(6)	17.01(12)	15.07(9)	17.88(13)	15.67(10)	18.38(13)	15.99(10)
$80k$	15.97(10)	14.51(8)	18.09(12)	15.97(10)	19.03(13)	16.63(10)	19.56(14)	16.98(11)
$120k$	17.18(16)	15.50(13)	19.6(12)	17.21(16)	20.6(2)	17.95(17)	21.2(2)	18.39(18)
$160k$	18.6(2)	16.63(18)	21.2(3)	18.6(2)	22.4(3)	19.5(2)	23.1(3)	19.9(2)
$240k$	20.0(2)	17.92(18)	23.0(3)	20.1(2)	24.3(3)	21.0(2)	25.0(3)	21.6(2)

namely, the effective curvature radius ρ_{eff} of the sphere that best fits the data.⁶ Note that the continuum functions \bar{d}/δ follow universal curves like those depicted in Fig. 3 when written in terms of rescaled distances δ/ρ , where ρ is the curvature radius of the spherical or hyperbolic space in question. Since \bar{d}/δ at a given point must be computed by numerical integration, to save on computational resources we did this calculation once for each of the 100 evenly spaced values $\delta/\rho \in [0, 2\pi]$, and used linear interpolation to compute \bar{d}/δ for arbitrary δ and ρ . The integrations over the sphere pairs were done with MATHEMATICA for $D \leq 4$, and with the help of a small program implementing Monte Carlo importance sampling for the case $D = 5$. We then performed χ^2 fits on the set of data points with $\delta > 5$ to determine the optimal curvature radius ρ_{eff} minimising χ^2 . To this end, we sampled ρ -values in discrete intervals of 0.01 for $N = 20k$ and $30k$ and 0.1 for all larger volumes.

Figure 4 includes a fit of the data for $N = 40k$ to a four-dimensional sphere, obtained by using an additive shift and $\rho_{\text{eff}} = 16.7$ in units of edge length. Given the highly nonclassical nature of the underlying geometry, a perfect fit to the given functional form could have hardly been expected, but considering this circumstance the closeness of the fit is still quite remarkable.

Our results for the effective curvature radii for volumes of up to $240k$, using both additive and multiplicative shifts, and fitting to spheres of dimension up to five, are collected in Table I. Since the shapes of the continuum curves for \bar{d}/δ in the region sampled are rather similar for different dimensions D (cf. Fig. 5), the quality of the fits, measured in terms of the mean squared deviation, does not depend strongly on D , although it does become slightly better as D increases. Also, using an additive instead of a multiplicative shift improves the fit quality slightly. As an illustration, the mean squared deviation for $N = 40k$ and $D = 5$ is 0.0392 for the multiplicative shift and 0.0379 for the additive shift.

⁶The sectional curvature of round spheres in any dimension is $1/\rho^2$.

The difference is small, but systematic and of similar magnitude for other volumes and dimensions.

Two more observations can be extracted from Table I. First, the effective curvature radius ρ_{eff} becomes larger when we increase the dimension of the sphere that is being fitted to, while keeping the discrete volume fixed. The likely explanation is that the continuum curves for higher D are initially steeper (cf. Fig. 5), which is also achieved by having a larger ρ_{eff} . Second, ρ_{eff} is systematically larger (on the order of 10–15%) when using an additive rather than a multiplicative shift. At this stage, this is simply a piece of information to be taken on board, because we do not have good theoretical arguments to prefer one type of shift over the other.

Next, we need to investigate the behavior of the quantum Ricci curvature as a function of the volume N , and gather evidence of whether a scaling limit exists as $N \rightarrow \infty$. For the comparison with continuum spheres to be meaningful, we expect that a rescaling of δ by the effective curvature radius for a given N will be needed. Working with $D = 5$ and an additive shift for definiteness, the general situation is illustrated well by Fig. 6, which shows the expectation

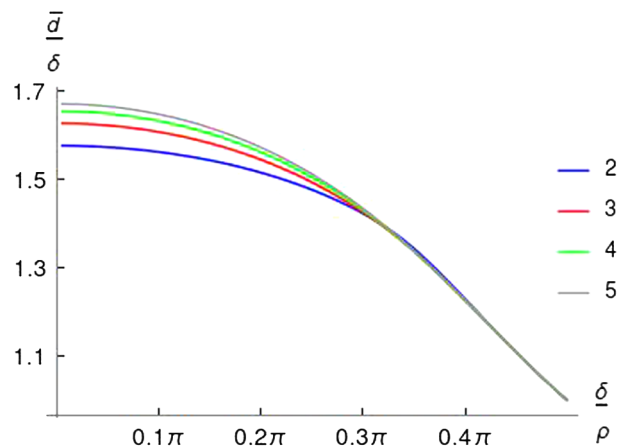


FIG. 5. Comparing normalized average sphere distances for continuum spheres in dimensions $D = 2, \dots, 5$ (bottom to top), covering the range $\delta/\rho \lesssim 0.4\pi$ in normalized distances, which is also explored in the Monte Carlo simulations.

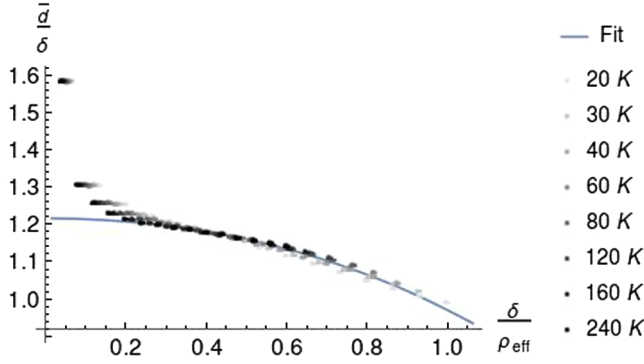


FIG. 6. Measurements of the normalized average sphere distance as a function of the rescaled distance δ/ρ_{eff} , for volumes in the range $N \in [20k, 240k]$, with the best fit to a five-dimensional continuum sphere. (Error bars are too small to be visible).

values $\langle \bar{d}/\delta \rangle$ as a function of the rescaled distance δ/ρ_{eff} for a wide range of discrete volumes. The optimal shift of the continuum curve was determined by removing all data points with $\delta < 5$ and then performing a joint fit to the remaining data. Beyond the region of lattice artifacts for small distances, the data points settle down to a common curve in an intermediate regime. Their observed slight spread for larger values of δ/ρ_{eff} is expected due to the presence of finite-size effects. This should be most pronounced for the simulations at smaller volume, which is in agreement with our data. We conclude that our measurements provide good evidence that in the continuum limit of two-dimensional dynamical triangulations of spherical topology, the quantum Ricci curvature $\langle K_q \rangle$ is a well-defined finite quantity with a nontrivial scale dependence, and is positive in the range of δ/ρ considered.

Assuming that the data for the largest volume $N = 240k$ represent a good approximation of the infinite- N behavior of the observable $\langle \bar{d}/\delta \rangle$, the match with the continuum curve is remarkably good. It is not perfect, due to a slight “overshoot” of the measurements at the largest values of δ/ρ_{eff} we considered. However, since there is no reason to believe that the DT quantum geometries behave like smooth round spheres in terms of *all* their metric properties, this is not particularly surprising.

Since the quality of the sphere fits and the scaling behavior as a function of volume show only a slight dependence on the dimension D of the spheres, we have performed an additional measurement to determine which value of D describes the curvature properties of the quantum geometry best. The criterion we use is motivated by the property of round D -dimensional spheres in the continuum, whose volume V scales with the D th power of the curvature radius ρ , $V(\rho) \propto \rho^D$. If the dynamically triangulated quantum geometry indeed resembles a D -dimensional sphere globally, one would expect that its effective curvature radius scales with the corresponding fractional power, that is,

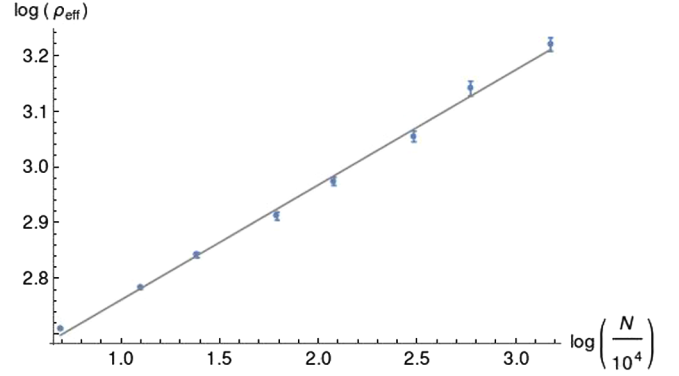


FIG. 7. Log-log plot of the effective radius ρ_{eff} as a function of the volume N , together with a linear fit, leading to $\mathcal{D} = 4.85(16)$. In the case shown, ρ_{eff} was extracted from fitting to a five-sphere (i.e., $D = 5$) and using an additive shift.

$$\rho_{\text{eff}} \propto N^{\frac{1}{\mathcal{D}}}. \tag{7}$$

We have examined all eight cases listed in Table I in search of power-law behavior of the form (7). We look for consistent pairs of D and \mathcal{D} , where the two dimensions agree. To extract the dimension \mathcal{D} , we fitted the data in each case to a straight line in a log-log plot. An example is depicted in Fig. 7, for $D = 5$ and using an additive shift in the sphere matching. As illustrated by the case shown, the quality of the linear fits is generally good. The complete set of results is listed in Table II. From its entries, we conclude that the only consistent case is that of five dimensions, where D and \mathcal{D} agree within error bars, for either choice of shift.

Last, one interesting aspect of the (quasilocal) quantum Ricci curvature—inherited from its classical, tensorial counterpart—is that it allows us in principle to capture some directional properties of curvature. Note that this is already true in dimension two. We have performed a small exploratory study for $N = 40k$ and $\delta = 15$ on two-dimensional dynamical triangulations, to try and understand whether the high degree of anisotropy of the geometry *at a given vertex of a given DT configuration* (due to its “baby-universe structure”) leaves an imprint on the curvature measurements. To this end, we considered the δ -sphere S_p^δ around some fixed vertex p and measured the

TABLE II. Dimension \mathcal{D} extracted from the scaling law (7) for the effective curvature radius ρ_{eff} , with ρ_{eff} obtained from fitting to a D -dimensional continuum sphere, using an additive (“+”) or multiplicative (“×”) shift.

D from sphere fit	$\mathcal{D}, +$	\mathcal{D}, \times
2	5.7(3)	6.0(3)
3	5.02(17)	5.21(17)
4	4.92(17)	5.04(15)
5	4.85(16)	4.94(14)

distribution of the average sphere distance $\bar{d}(\delta)$ to all spheres $S_{p'}^\delta$ with center p' on the sphere S_p^δ . In this manner one explores all directions around the point p . A signal of anisotropic behavior would be if the average sphere distances clustered around two or more distinct values. However, after taking suitable averages of the measured directional distributions to get rid of the vertex dependence, we found that the resulting average distribution is approximately Gaussian with a single peak. It suggests that, at least for distances of the order of $\delta/\rho \approx 1$, this quantity behaves perfectly isotropically, further illustrating the robustness of quantum Ricci curvature as a quantum observable.

IV. SUMMARY AND OUTLOOK

We set out to evaluate a recently introduced geometric quantum observable—the quantum Ricci curvature—in two-dimensional quantum gravity defined by dynamical triangulations. The quantity measured directly in the Monte Carlo simulations was the expectation value $\langle \bar{d}/\delta \rangle$ of the normalized average sphere distance, from which the quantum Ricci curvature $\langle K_q(\delta) \rangle$ can be extracted via a quantum analogue of Eq. (2).

A qualitative inspection of the data $\langle \bar{d}/\delta \rangle(\delta)$ signaled a positive curvature in the δ range considered. This motivated a further quantitative comparison with smooth classical model spaces of constant positive curvature, given by round spheres of dimension D . For given $D \in \{2, 3, 4, 5\}$, we extracted the curvature radius of the sphere that best fitted the Monte Carlo data, for a total of eight different system sizes $N \leq 240000$. The effective curvature radii thus obtained (Table I) allowed us to perform a scaling analysis for a given D , by plotting the measured data as a function of the rescaled distances δ/ρ_{eff} . The rescaled data display only a mild N dependence, and provide good evidence for the existence of a universal curve $\langle \bar{d}/\delta \rangle$ as $N \rightarrow \infty$. We noted that the quality of the fits to curves for continuum spheres becomes slightly better as the dimension D increases. Unlike what one might have expected naively in a theory of two-dimensional quantum gravity, $D = 2$ therefore appeared to be the least preferred of the integer values we considered.

To extract a “best dimension” associated with the quantum Ricci curvature construction, we then investigated a complementary criterion for measuring a dimension, by looking at the dependence of the effective curvature radii on the system size. Since the Hausdorff dimension of DT quantum gravity is four, a natural conjecture would be that the preferred sphere dimension to emerge from the curvature analysis is also four. Instead, it turned out that the preferred, self-consistent dimension associated with the numerical data gathered is five. This noncanonical behavior

underscores the fact that the dynamically generated quantum geometry of the model is highly nonclassical and does not resemble any given smooth geometry.

We cannot offer a more specific interpretation of the value five at this stage, because DT quantum gravity in two dimensions is currently the only nonperturbative quantum model whose quantum Ricci curvature has been analyzed. In addition, the model does not have a conventional classical limit one could use for comparison, because there is no classical theory of general relativity in two spacetime dimensions. It would be very interesting to understand whether the quantum Ricci curvature can be derived analytically in one of the various descriptions of two-dimensional Euclidean quantum gravity that are available [10,14].

An important aspect of the present work is the demonstration that the quantum Ricci curvature can be implemented in nonperturbative quantum gravity in a rather straightforward way. Although we did not consider the full-fledged theory in four dimensions, the two-dimensional model we examined is of particular interest because of the highly nonclassical nature of its quantum geometry, far removed from the spaces we considered earlier [9]. As an added “bonus” we found the unexpected result that its quantum Ricci curvature follows closely that of a smooth five-sphere.

In summary, we have established by way of a nontrivial example that *quantum Ricci curvature* is a well-defined quantum observable, giving us a new, independent way to quantify the properties of quantum geometry. Given the general dearth of observables in quantum gravity, this is an important result. It opens a variety of avenues for further exploration, most importantly the application to full non-perturbative (CDT) quantum gravity in four spacetime dimensions (as outlined in Sec. I), which is currently under way. However, any formulation of quantum gravity that uses discrete building blocks with suitable metric properties to describe space(time) should provide a natural habitat for quantum Ricci curvature. Among the other interesting aspects to be understood, also in lower dimensions, is the interplay between local and global properties, more specifically, the influence of global topology and boundary conditions on the quantum Ricci curvature. We hope to return to this issue in the near future.

ACKNOWLEDGMENTS

This work was partly supported by the research program “Quantum gravity and the search for quantum spacetime” of the Foundation for Fundamental Research on Matter (FOM, now defunct), financially supported by the Netherlands Organisation for Scientific Research (NWO).

- [1] J. Ambjørn, A. Görlich, J. Jurkiewicz, and R. Loll, Non-perturbative quantum gravity, *Phys. Rep.* **519**, 127 (2012).
- [2] J. Ambjørn and K. N. Anagnostopoulos, Quantum geometry of 2D gravity coupled to unitary matter, *Nucl. Phys.* **B497**, 445 (1997).
- [3] J. Ambjørn, A. Görlich, J. Jurkiewicz, and R. Loll, Planckian birth of the quantum de Sitter universe, *Phys. Rev. Lett.* **100**, 091304 (2008); The nonperturbative quantum de Sitter universe, *Phys. Rev. D* **78**, 063544 (2008).
- [4] J. Ambjørn, J. Jurkiewicz, and R. Loll, Emergence of a 4D world from causal quantum gravity, *Phys. Rev. Lett.* **93**, 131301 (2004); Reconstructing the universe, *Phys. Rev. D* **72**, 064014 (2005).
- [5] J. Ambjørn, J. Jurkiewicz, and R. Loll, Spectral dimension of the universe, *Phys. Rev. Lett.* **95**, 171301 (2005).
- [6] J. Ambjørn, J. Gizbert-Studnicki, A. Görlich, and J. Jurkiewicz, The effective action in 4-dim CDT. The transfer matrix approach, *J. High Energy Phys.* **06** (2014) 034; J. Ambjørn, J. Gizbert-Studnicki, A. Görlich, J. Jurkiewicz, N. Klitgaard, and R. Loll, Characteristics of the new phase in CDT, *Eur. Phys. J. C* **77**, 152 (2017).
- [7] J. Ambjørn, A. Görlich, J. Jurkiewicz, A. Kreienbuehl, and R. Loll, Renormalization group flow in CDT, *Classical Quantum Gravity* **31**, 165003 (2014).
- [8] J. Ambjørn, S. Jordan, J. Jurkiewicz, and R. Loll, A second-order phase transition in CDT, *Phys. Rev. Lett.* **107**, 211303 (2011); Second- and first-order phase transitions in CDT, *Phys. Rev. D* **85**, 124044 (2012).
- [9] N. Klitgaard and R. Loll, Introducing quantum Ricci curvature, *Phys. Rev. D* **97**, 046008 (2018).
- [10] J. Ambjørn, B. Durhuus, and T. Jonsson, *Quantum Geometry: A Statistical Field Theory Approach* (Cambridge University Press, Cambridge, England, 1997).
- [11] H. Kawai, N. Kawamoto, T. Mogami, and Y. Watabiki, Transfer matrix formalism for two-dimensional quantum gravity and fractal structures of space-time, *Phys. Lett. B* **306**, 19 (1993); J. Ambjørn and Y. Watabiki, Scaling in quantum gravity, *Nucl. Phys.* **B445**, 129 (1995).
- [12] J. Ambjørn, J. Jurkiewicz, and Y. Watabiki, On the fractal structure of two-dimensional quantum gravity, *Nucl. Phys.* **B454**, 313 (1995).
- [13] Y. Ollivier, Ricci curvature of Markov chains on metric spaces, *J. Funct. Anal.* **256**, 810 (2009).
- [14] F. David, Simplicial quantum gravity and random lattices, in *Gravitation and Quantizations*, edited by B. Julia and J. Zinn-Justin (North-Holland, Amsterdam, 1995), p. 679; P.H. Ginsparg and G.W. Moore, Lectures on 2-D gravity and 2-D string theory, in *Recent Directions in Particle Theory*, edited by J. Harvey and J.G. Polchinski (World Scientific, Singapore, 1993), p. 277.